Journal of Physical Chemistry & Biophysics

Lue, et al., J Phys Chem Biophys 2015, 5:3
DOI: 10.4172/2161-0398.1000181

Research Article Open Access

Correlation between Dye-Sensitized Solar Cell Performance and Internal Resistance using Electrochemical Impedance Spectroscopy

Lue SJ[1,*], Lo PW[1], Huang FY[1], Cheng KW[1] and Tung YL[2]

[1]*Department of Chemical and Materials Engineering and Green Technology Research Center, Chang Gung University, Kwei-shan, Taoyuan 333, Taiwan*
[2]*Green Energy and Environment Research Laboratories, Industrial Technology Research Institute (ITRI), Hsin-Chu 310, Taiwan*

Abstract

Dye sensitized solar cells (DSSCs) containing 3-methoxypropionitrile (MPN) electrolyte solution are prepared by introducing microporous polycarbonate (PC) film supports of two pore sizes (nominal diameters of 0.2 and 0.05 μm). These PC films are stable up to 400°C. The conductivities of the PC films impregnated with the MPN electrolyte solution are not significantly different from each other. The DSSC efficiencies with and without the PC supports are compared under illumination intensities of 20, 50, and 100 mW cm-2. Under medium to strong light intensity, the control cell (without PC supports) has the highest photo-to-current efficiency, followed by those with the 0.2 and 0.05 μm PC supports. In the low intensity incident light, the cells with the 0.2 μm support slightly outperform the other cells. The control DSSCs and DSSCs containing PC supports are aged via light soaking at 60°C. The as-prepared and aged cells are analyzed using electrochemical impedance spectroscopy to isolate resistance components in the DSSCs. The cell efficiency is highly correlated with the reciprocal of serial resistance, which is the sum of the resistance values resulting from the platinum counter electrode, the ionic diffusion in the electrolyte, and the sheet resistance of the transparent conducting oxide. The resistance due to the ionic diffusion in the electrolyte is the most profound contributor to the serial resistance in the aged cells.

Keywords: Accelerated aging of dye sensitized solar cells (DSSCs); 3-methoxypropionitrile (MPN); Long-term cell performance; Electrochemical impedance spectroscopy (EIS)

Introduction

Solar cells are a rapidly growing research topic and a promising substantial renewable energy source. Among the several types of solar cells, dye-sensitized solar cells (DSSCs) have the advantages of low-cost, environmentally friendly manufacturing process, high photon-to-electron conversion efficiency under low light intensity, and facile fabrication into flexible panels [1-3].

A typical DSSC consists of conductive transparent glass with nano-structured mesoscopic TiO_2, a light harvesting dye, and an redox couple (e.g., I^-/I_3^-) electrolyte in an organic solvent (e.g., acetonitrile, AN). Pt-coated conductive glass is used as the counter electrode [1-4]. One of the challenges of DSSCs is lifetime. The liquid electrolytes suffer from liquid volatilization and leakage, thus reducing the cell efficiency and eventually shortening the cell lifetime. Research on improving electrolyte stability includes the use of solid or gel electrolyte [5-8], replacing the volatile solvents with ionic liquids [9-11], and incorporating polymeric films into DSSCs [12-16]. Ion diffusivity is slower in solid electrolytes and ionic liquids. Therefore, the use of micro-porous films as the framework material seems to have potential due to the film's solvent retention capabilities achieved by the capillary force exerted between the porous support and the liquid [17].

In previous publications [17,18] we demonstrated the use of micro-porous polycarbonate (PC) or alumina (Al_2O_3) as framework materials in AN-based electrolyte solution between the TiO_2 working electrode and the platinum (Pt) counter electrode. The framework materials provide sufficient ion transport paths and help to retain the electrolyte solution by preventing evaporation loss. The long-term stability was greatly enhanced by incorporation of the supports [17,18].

In addition to AN, 3-methoxypropionitrile (MPN) has been widely adopted as a solvent in DSSCs for its lower volatility [19], lower toxicity, and better chronological photovoltaic performance stability [20]. Wang et al. prepared DSSC containing an amphiphilic ruthenium sensitizer in conjunction with an MPN-based polymer gel electrolyte, reaching an efficiency of >6% in full sunlight (air mass 1.5, 100 mW cm^{-2}). This device was able to sustain heating for 1,000 h at 80°C, maintaining 94% of its initial performance [21]. Gratzel examined the temporal evolution of photovoltaic parameters of DSSCs using a new amphiphlic sensitizer (K19), with decylphosphonic acid (DPA) as co-adsorbent and a novel electrolyte formulation (0.8M 1-propyl-3-methylimidazolium iodide, 0.15M I_2, 0.1M guanidinium thiocyanate, and 0.5M n-methylbenzimidazole in MPN). The device showed an excellent stability under the dual stress of heating and visible light soaking of 1000 h, retaining 97.7% of its initial power conversion efficiency [22]. Recently Flasque et al. reported a uniform solid electrolyte interphase (SEI) layer formed around the TiO_2 semi-conductor surface in the presence of a MPN solvent. The chemical composition of this SEI resulted from the solvent and additive degradation. The SEI thickness, its content, and the concentration profile strongly depended on the ageing conditions [23].

The objective of this work is to investigate the DSSC efficiency by incorporating micro-porous polycarbonate (PC) films of different pore sizes into MPN-based DSSCs. The cell efficiencies of the prepared DSSCs with and without the PC films under various illumination intensities were compared. The long-term cell performance, including the photo-current density (J_{sc}), open-circuit voltage (V_{oc}), fill factor

***Corresponding author:** Lue SJ, Department of Chemical and Materials Engineering and Green Technology Research Center, Chang Gung University, Kwei-shan, Taoyuan 333, Taiwan, Tel: 886-3-2118800, extn. 5489; E-mail: jessie@mail.cgu.edu.tw

Received April 27, 2015; **Accepted** June 10, 2015; **Published** June 14, 2015

Citation: Lue SJ, Lo PW, Huang FY, Cheng KW, Tung YL (2015) Correlation between Dye-Sensitized Solar Cell Performance and Internal Resistance using Electrochemical Impedance Spectroscopy. J Phys Chem Biophys 5: 181. doi:10.4172/2161-0398.1000181

(FF), and light-to-electrical energy conversion efficiency, was recorded for as-prepared cells and cells aged in a light-soaking chamber for up to 650 hours. The internal resistances of the DSSCs with and without PC supports and with various aging times were analyzed using electrochemical impedance spectroscopy (EIS). The cell efficiency was correlated with the overall cell resistance, and the major resistance contributor was determined. The role of the PC supports during the DSSC aging process was also elucidated.

Experimental

Materials

The fluorine-doped tin oxide (FTO) conductive glass (resistance=7 Ω cm^{-2}) was from NSG America Inc. (Somerset, NJ, USA). The ruthenium 535 bis-TBA (N 719) dye was obtained from Dyesol Ltd. (Queanbeyan, Australia). AN, iodine (I_2, purity of 99.9%), and isopropyl alcohol (IPA) were obtained from JT Baker (Phillipsburg, NJ, USA). Tert-butanol (99%), acetone, lithium iodide hydrate (LiI, 99.99%), 1-methylbenzimidazole (NMBI, 99%), MPN (98%), and hydrogen hexachloroplatinate (IV) hydrate (H_2PtCl_6) were purchased from Aldrich (St. Louis, MO, USA). 1-methyl-3-propylimidazolium iodide (PMII) was synthesized by the Photovoltaics Technology Center at the Industrial Technology Research Institute (ITRI), Taiwan. The hot melt sealing foil (SX1170-60) was from Solaronix SA (Aubonne, Switzerland). The colloidal silver liquid was purchased from Ted Pella Inc. (Redding, CA, USA). The photo-curing compound (GN435) was purchased from ever wide Chemical Co. Ltd. (Douliou, Taiwan). The polycarbonate (PC) films with nominal pore sizes of 0.2 and 0.05 μm were purchased from Whatman Ltd. (London, UK).

PC film characterization

The dry thicknesses of the PC films were measured using a thickness gauge (Elcometer® 345, Elcometer Inc., Manchester, UK). The pore size distribution was measured using capillary flow porometry (Porous Materials, Inc., Ithaca, NY, USA) with Galwick (surface tension of 15.9 dynes cm^{-1}) as the wetting solvent. The PC film sample was analyzed using the wet up/dry down mode. The porosity was determined using the mean pore size data. Field-emission scanning electron microscopy (FESEM, model S-4800, Hitachi Ltd., Tokyo, Japan) was used to characterize the actual pore sizes and surface and cross-sectional morphologies of the gold-coated PC films with different nominal pore sizes (0.05 and 0.2 μm). Twenty kV voltage and 75 μA current were used during the FESEM operation. The thermal stability was measured on a thermal gravimetric analyzer/mass spectrometer (TGA/MS, model STA 409CD/QUADSTAR-422, Netzsch, Selb, Germany). The sample was heated at a rate of 10°C min^{-1} under a helium atmosphere.

The PC film was immersed in the electrolyte solution for 24 hours, and the resistance and conductivity were measured using a potentiostat/galvanostat (Autolab PGSTAT302N, Metrohm Autolab B.V., Utrecht, Netherlands) [24,25]. The thickness of the swollen film was measured to determine the dimensional stability [26]. The chemical compatibility was performed by weighing the PC film before and after immersion in pure MPN solvent.

The bulk resistance was determined from the Nyquist plot of the electrolyte-impregnated PC film according to the procedure described in the literature [25]. The conductivity (σ, in S cm^{-1}) of the electrolyte-impregnated PC film was calculated using the following equation:

$$\sigma = \frac{l}{R_b A} \quad (1)$$

Where l is the thickness of the electrolyte-impregnated PC film (cm), R_b is the bulk resistance (Ω), and A is the contact area of the stainless steel electrodes (cm^2).

DSSC and dummy cell preparation

FTO conductive glass of 2.5 × 1.5 cm was used as the electrode substrate. The photo-catalytic TiO_2 paste was synthesized by ITRI and screen-printed onto the FTO substrate with an active area of 0.28 cm^2. The electrode was heated to 400°C for 20 min. The electrode was immersed in a 5×10^{-4}M solution of N 719 dye in AN/tert-butanol (1:1 v/v) solution at 60°C for 3 h to adsorb the dye molecules. The electrode was rinsed with acetone to remove excess dye solution and dried at 80°C for 2 min.

The counter electrode was prepared by screen-printing with H_2PtCl_6 (0.015M in IPA) on another piece of FTO glass in which two holes were drilled. The Pt counter electrode was annealed at 400°C for 20 min and gradually cooled to room temperature for 10 min. The PC film was carefully aligned between the TiO_2 electrode and the counter electrode. Then, a hot melt sealing foil was used to seal the DSSC using hot-pressing at 130°C for 40 s under 65 kN cm^{-2} pressure. The electrolyte solution (0.8M PMII/0.05M I_2/0.5M NMBI in MPN) was injected into one hole on the counter electrode. The holes were sealed using ultraviolet (UV) light after the photo-curing compound was placed in the holes and covered by a slide glass. The top and cross-sectional views of the assembled DSSC were reported previously [17]. Colloidal silver liquid was coated on the FTO glasses of the working and counter electrodes and air-dried prior to photovoltaic measurement.

Dummy cells were assembled for the solvent evaporation test. Two screen-printed Pt electrodes attached onto clean FTO glasses were used to assemble dummy cells. In some dummy cells, the PC films were inserted and aligned between the Pt electrodes before the cells were sealed with hot melted sealing foil. The other dummy cells contained liquid electrolyte solution alone. The electrolyte solution (0.8M PMII/0.05M I_2/0.5M NMBI in MPN) was injected into the cell gap through one drilled hole on the Pt electrode. The two drilled holes in the FTO glasses were not sealed to expedite the drying process. The tested cell was placed onto the weight pan of a micro-balance (CP2225D, Sartorius, Goettingen, Germany). The weight loss was recorded at time intervals.

Photovoltaic efficiency of DSSC

The assembled DSSC performance was measured at room temperature under illumination of 20-100 mW cm^{-2} (Xenon lamp power supply, model YSS-100A, Yamashita Denso Corporation, Tokyo, Japan). The cell was first activated for 20 min, and the photocurrent and voltage were recorded. The as-prepared and aged DSSCs were tested for long-term stability. The cells were aged in a light soaking chamber of 100 mW cm^{-2} (1 sun, AM 1.5) at 60°C and 5% relative humidity (xenon weather-ometer, model Ci3000, SDL Atlas, Rock Hill, SC, USA). The cell voltage and current density relationship was determined using a linear sweep voltammetry on a potentiostat (pgstat3, Autolab, ECO chemie B. V., Utrecht, Netherlands). The efficiency (η) of each DSSC was determined using Eq. (2)

$$\eta = \frac{V_{oc} \times J_{sc} \times FF}{P_{in}} \times 100\% \quad (2)$$

Where V_{oc} is open-circuit voltage (the maximum voltage value), J_{sc} is short-circuit current density (the maximum current density value), P_{in} is incident light power, and FF is fill factor. FF was determined using Eq. (3):

$$FF = \frac{J_{\max} V_{\max}}{J_{sc} V_{oc}} \quad (3)$$

Where J_{max} and V_{max} are the current and voltage values, respectively, which give the maximum *JV* product value.

Internal resistance of DSSC

The internal resistance of the DSSC was determined using electrochemical impedance spectroscopy (EIS), and the value was partitioned into contributions from various components. The cell was scanned at a frequency between 0.1 and 10^5 Hz with 10 mV of potential applied across the electrodes. On the impedance spectrum of a DSSC, three semicircles are observed in the measured frequency range of 10^{-1}-10^5 Hz. The semicircles in the frequency regions 10^3-10^5, 1-10^3, and 0.02-1 Hz are attributed to impedance related to charge-transfer processes occurring at the Pt counter electrode (R_{CE}), at the TiO_2/dye/electrolyte interface (R_{TiO2}), and in Nernstian diffusion within the electrolyte (R_{ELE}), respectively. The resistance element R_H in the high frequency range of $>10^5$ Hz is mainly due to the sheet resistance of FTO [27]. R_{TiO2} acts similarly to a diode's resistance, while R_{CE}, R_{ELE}, and R_H show series internal resistance behavior. The equivalent-circuit and resistance values of the components were obtained using the Fit & Simulation function in NOVA version 1.10.3 by the Frequency Response Analysis (FRA) software (Metrohm Autolab BV, Utrecht, Netherlands) [28]. The serial resistance of the entire DSSC (R_S) equals the sum of R_H, R_{CE}, and R_{ELE}.

Results and Discussion

PC film characterization

The surface morphologies of the PC support films obtained using FESEM are shown in Figures 1a and 1b. The pores were cylindrical and aligned at a perpendicular orientation to the film surface. This means the pore tortuosity was close to unity, which is beneficial for ion transport in the electrolyte incorporated with the PC films. The narrow pore size distributions of the 0.2 μm and 0.05 μm PC films are illustrated in Figures 1c and 1d, respectively. Because there were adjacent pores connected to each other (Figure 1a) for the 0.2 μm PC film, a large portion of the average pore size was in the 0.22-0.24 μm range (Figure 1c).

The average dry film thickness was 3.50 μm for the 0.05 μm PC film and 5.62 μm for the 0.2 μm PC film. The MPN-swollen film thickness increased to 4.40 μm for the 0.05 μm PC film and 5.74 μm for the 0.2 μm PC film. There was negligible weight loss of the PC film in the MPN solvent, indicating insignificant polymer dissolution in the organic solvent. The thermal stability of the PC film was tested using TGA. The PC film was stable up to 440°C. The main degradation temperature occurred at 480°C. This high thermal stability ensures that the PC support can withstand the operation temperature under strong sunlight conditions.

The sub-micron sized PC films are expected to retain electrolyte solvent and prolong DSSC lifetime. Some dummy cells filled with electrolyte and some cells with PC films were tested for solvent loss over time. The results shown in (Figure 2) demonstrate that the liquid electrolyte alone had the highest solvent loss rate (9.72×10^{-4} mg min^{-1}). The addition of the 0.2 μm and 0.05 μm PC films helped with solvent

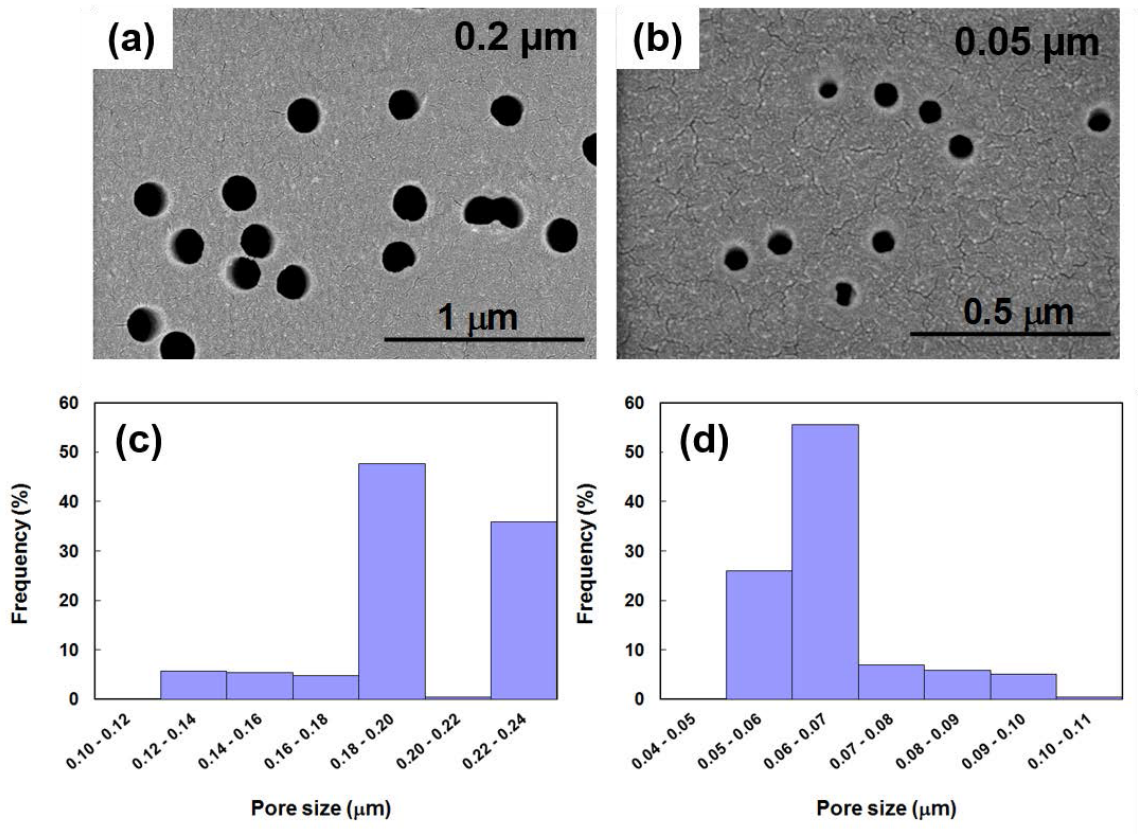

Figure 1: SEM micrographs of **(a)** 0.2 m and **(b)** 0.05 μm PC films and pore size distributions of **(c)** 0.2 μm and **(d)** 0.05 μm PC films.

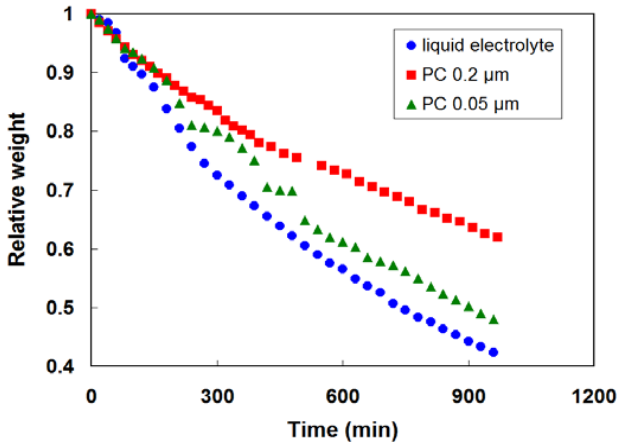

Figure 2: Solvent loss over time for dummy cells filled with liquid electrolyte and cells containing 0.2 m and 0.05 µm PC films (temperature=26 ± 1°C).

retention, and the solvent loss rates were reduced to 5.82×10^{-4} and 7.15×10^{-4} mg min^{-1}, respectively. The PC film supports were able to minimize solvent evaporation by withholding solvent in the pore cavities through capillary force.

The PC supports were impregnated with the electrolyte solution (0.8M PMII/0.05M I_2/0.5M NMBI in MPN), and the conductivities were measured. A typical Nyquist plot is shown in (Figure 3), and the resistance (R_b) was taken as the x-intercept of the extrapolated line (as shown in the inset of Figure 3). The conductivity was calculated with equation 1 [24-29]. Based on duplicate samples, the conductivity data were 0.607 ± 0.0141 and 0.620 ± 0.0148 S cm^{-1} for the 0.2 µm and 0.05 µm films, respectively. There was no statistically significant difference between the electrolyte-filled PC films.

DSSC performance

Replicate DSSCs were prepared and tested for photon-to-electron conversion efficiency under various light intensities. The original J-V curves are shown in (Figure 4), and these curves demonstrate good reproducibility. The control DSSCs (with electrolyte alone) exhibited a mean J_{sc} of 12 mA cm^{-2}, a mean V_{oc} of 0.76 V, a mean *FF* of 0.57, and a mean efficiency of 5.34% under 1 sun (100 mW cm^{-2}) (Table 1 and Figure 4a). As the light intensity decreased to 50 and 20 mW cm^{-2}, the mean J_{sc} significantly decreased to 5.8 and 0.77 mA cm^{-2}, respectively, and the mean V_{oc} slightly declined to 0.72 and 0.64 V, respectively, but the mean *FF* increased to 0.61 and 0.63, respectively (Table 1). The mean cell efficiency was reduced to 5.2 and 1.62% at an illumination intensity of 50 and 20 mW cm^{-2}, respectively.

For the DSSC containing the 0.2 µm PC film and illuminated at 1 sun, the J_{sc} and *FF* slightly decreased while the V_{oc} did not change, resulting in a lower efficiency (4.3%) versus the control cells. When this cell was exposed at medium light intensity (50 mW cm^{-2}), the cell efficiency was similar to the cell efficiency at 1 sun (Table 1). As the light intensity was further reduced to 20 mW cm^{-2}, the cell efficiency was reduced to 1.9%. The DSSCs containing the 0.05 µm PC film exhibited lower cell efficiency under various light intensities than the control cells and the cells containing the 0.2 µm PC film, mainly due to the lower J_{sc} values (Table 1). It is speculated that the 0.05 µm PC film had lower porosity than the 0.2 µm PC film (5% vs. 10%) and possessed lower surface area for ion diffusion between the electrodes. Therefore, the cell performance of the DSSCs with the 0.05 µm support was inferior to the cell performance of the DSSCs with the 0.2 µm support.

Long-term cell performance and electrical resistance

After the cell performance of the as-prepared DSSCs was analyzed, the cells were aged in a light soaking chamber. The cell efficiencies of the aged cells were measured again at various time intervals. The long-term cell performance is demonstrated in Figure 5. In the first 350 h, the control cells were stable with similar J_{sc}, V_{oc}, *FF* and efficiency. Beyond 350 h, the J_{sc} and the cell efficiency started to decline rapidly. The cells containing the PC supports exhibited lower J_{sc} and efficiency data than the control cells. Although the PC films helped solvent retention, the effective electrolyte hold-up volume was reduced. The decreased electrolyte volume became detrimental to long-term cell performance, especially in the continuous light soaking condition. The challenging condition of light soaking at 60°C made the dye instability and solvent loss worse. Therefore, the lifetime was shortened in the cells with PC films under continuous light illumination.

Electrical impedance spectroscopy (EIS) is a useful diagnostic tool to monitor and characterize in-situ inner DSSC phenomena [30,31]. To further elucidate the relationship between DSSC performance and the internal cell resistance, EIS analysis was performed on the as-prepared and aged cells. Typical impedance spectra for the as-prepared and aged DSSC containing 0.05 µm support are shown in Figure 6. The results for the control cells and those with PC films are summarized in Table 2. The fitted R_H values, which represent the conductivity resistance of the FTO glass, were in the range of 13.33 to 16.36 Ω for the fresh and aged DSSCs. In the as-prepared DSSCs, R_{TiO2} and R_{ELE} were higher in the PC-containing cells th0061n the control cells. This may be due to porous film steric hindrance creating tortuous diffusion paths for ion transport and reduced electrolyte holding volume. The remarkable

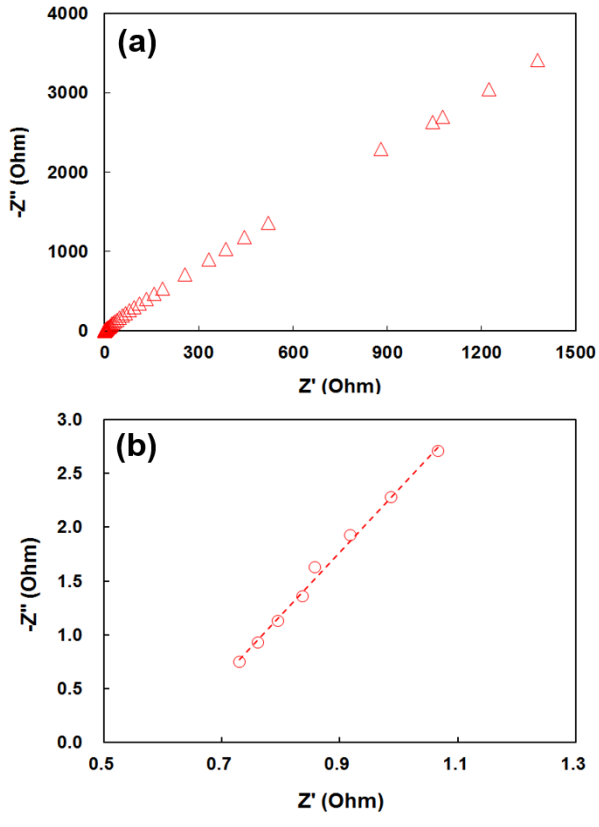

Figure 3: Nyquist plot **(a)** and enlarged high frequency region **(b)** for electrolyte-impregnated 0.2 µm PC film.

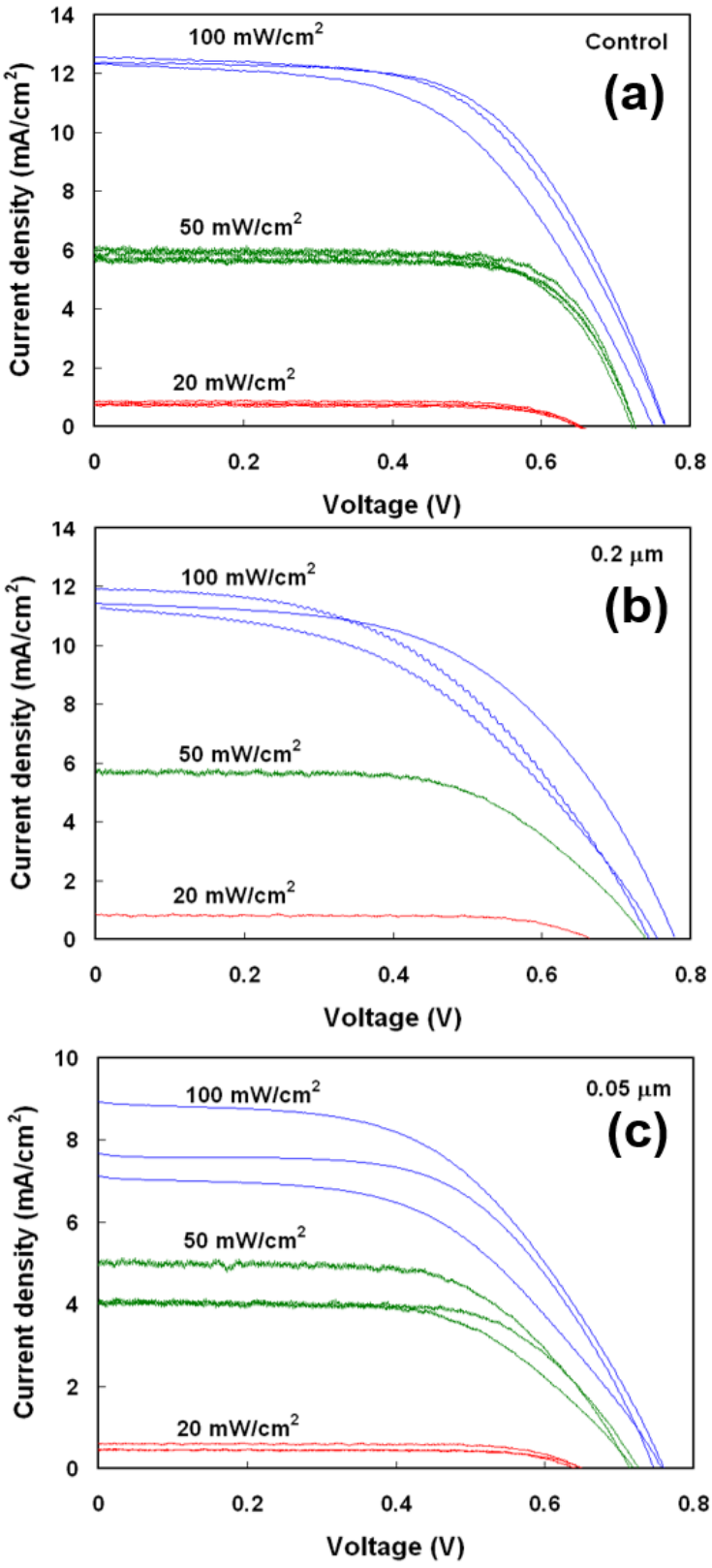

Figure 4: Current density-voltage curves for as-prepared DSSCs containing **(a)** control, **(b)** 0.2 μm PC film, and **(c)** 0.05 m PC film under various illumination intensities.

Illumination (mW cm^{-2})	Electrolyte support	J_{sc} (mA cm^{-2})	V_{oc} (V)	FF	Efficiency (%)
100	None	12.30 ± 0.12[b]	0.76 ± 0.01	0.57 ± 0.03	5.34 ± 0.36
100	0.2 μm PC film	11.470.31	0.76 ± 0.02	0.49 ± 0.04	4.29 ± 0.39
100	0.05 μm PC film	7.84 ± 0.92	0.76 ± 0.01	0.54 ± 0.03	3.17 ± 0.40
50	None	5.78 ± 0.13	0.72 ± 0.01	0.61 ± 0.02	5.18 ± 0.18
50	0.2 μm PC film	5.64	0.73	0.58	4.70
50	0.05 μm PC film	4.30 ± 0.50	0.71 ± 0.01	0.70 ± 0.04	4.25 ± 0.51
20	None	0.77 ± 0.05	0.64 ± 0.01	0.63 ± 0.01	1.62 ± 0.15
20	0.2 μm PC film	0.84	0.66	0.69	1.89
20	0.05 μm PC film	0.67 ± 0.27	0.64 ± 0.01	0.84 ± 0.02	1.34 ± 0.22

[a]Single-sealed cells with active area of 0.28 cm^2; electrolyte consisting of 0.8M PMII/0.05M I_2/0.5M NMBI in MPN.
[b]Mean ± standard deviation (N=3) except for 0.2 m PC film at 20 and 50 mW cm^{-2}.

Table 1: Cell performance of as-prepared DSSC[a] with and without PC films.

Electrolyte support	R_H (Ω)	R_{CE} (Ω)	R_{TiO2} (Ω)	R_{ELE} (Ω)
None (t=0)	13.65	15.90	13.71	9.11
0.2 μm PC (t=0)	14.11	15.99	36.20	12.17
0.05 μm PC (t=0)	15.42	15.67	44.30	22.43
None (t=648 h)	13.33	11.03	21.01	149.7
0.2 μm PC (t=648 h)	16.36	12.08	28.74	188.4
0.05 μm PC (t=648 h)	15.95	22.02	20.46	125.7

[a]Single-sealed cells with active area of 0.28 cm^2; electrolyte consisting of 0.8M PMII/0.05M I_2/0.5M NMBI in MPN.

Table 2: Resistance components in as-prepared and aged DSSCs[a] with and without PC films.

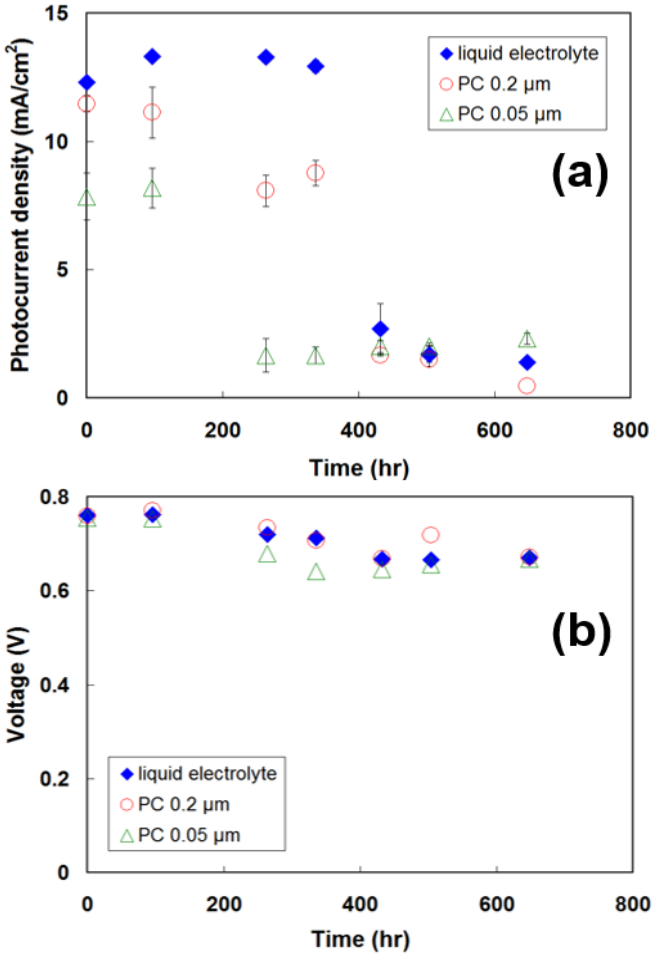

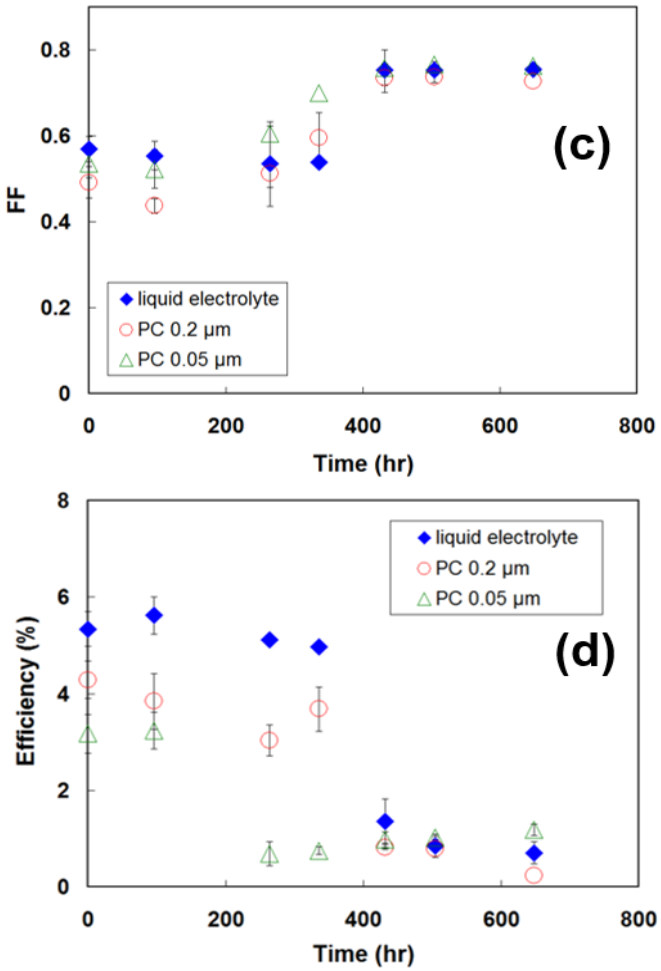

Figure 5: Variations in **(a)** short-circuit photocurrent density, **(b)** open-circuit voltage, **(c)** fill factor (FF), and **(d)** efficiency as a function of time for DSSCs assembled with liquid electrolyte and with PC microporous supports of different pore sizes. The solar cells were kept in light soaking (illumination of 100 mW cm^{-2}) at 60°C. Electrolyte composition was 0.8M PMII/0.05M I_2/0.5M NMBI in MPN.

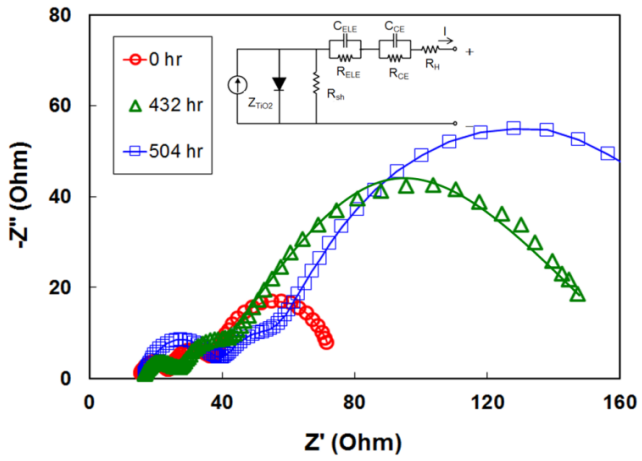

Figure 6: Electrochemical impedance spectra of DSSCs with 0.05 μm support at various aging times and equivalent circuit shown in the insert. The solar cells were aged in light soaking (illumination of 100 mW cm^{-2}) at 60°C. Electrolyte composition was 0.8M PMII/0.05M I2/0.5M NMBI in MPN.

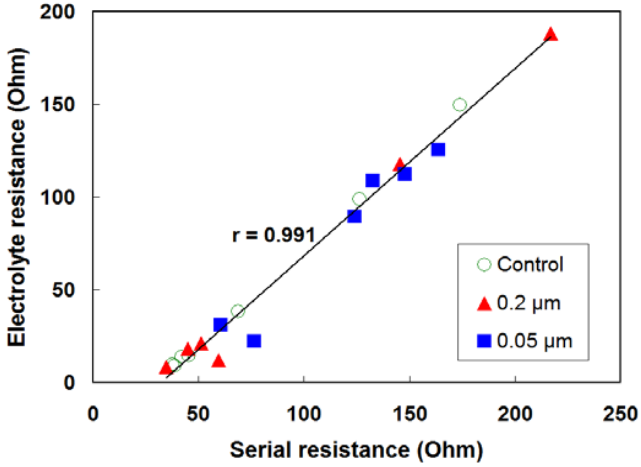

Figure 7: Strong linear relationship between serial resistance and resistance for electrolyte diffusion for all as-prepared and aged DSSCs. The solar cells were aged in light soaking (illumination of 100 mW cm^{-2}) at 60°C. Electrolyte composition was 0.8M PMII/0.05M I_2/0.5M NMBI in MPN.

findings in the aged cells are the significant increases in R_{ELE} values for the PC film-containing samples. This may be associated with the solvent evaporation or the sorption onto the PC supports.

The cell serial resistance, which is the sum of R_H, R_{CE}, and R_{ELE}, was recorded for all of the as-prepared and aged cells. The cell efficiency showed an inverse relationship with the serial resistance or a linearly increasing relationship with the reciprocal of the serial resistance. Among the serial resistance contributors, the electrolyte resistance (R_{ELE}) was found to have the most dominant role. The correlation coefficient between R_{ELE} and R_S was as high as 0.991 (Figure 7), indicating R_{ELE} was the most important factor in the long-term cell efficiency.

Conclusion

Porous PC films were incorporated into DSSCs, and the cell performance was evaluated. The PC supports were thermally stable and suppressed the electrolyte solvent evaporation rate. The as-prepared control cells (without PC film) yielded higher efficiencies at an illumination intensity of 100 mW cm^{-2} than the cells with the PC films. Under a low illumination intensity of 20 mW cm^{-2}, the DSSC with the 0.2 μm PC outperformed the control cells. The 0.05 μm PC film had a low porosity and contained the least amount of electrolyte solution, resulting in the lowest J_{sc} and efficiency among the tested cells.

As the DSSCs were prematurely aged via light soaking at 60°C, the cell efficiency declined with time. The photovoltaic efficiency of the aged cell showed an inverse relationship with the serial resistance, which was the sum of the last three aforementioned resistance components. In addition, the electrolyte resistance was found to have the most dominant role on the serial resistance with a correlation coefficient of 0.991.

Acknowledgement

We acknowledge the financial supports of the National Science Council of Taiwan (NSC 101-3113-E-182-001-CC2) and the Bureau of Energy, Ministry of Economic Affairs (102-D0607). We would also like to express gratitude to ITRI for technical support in the preparation of the TiO_2, the dye solution, and the counter electrode.

References

1. O'Regan B, Grätzel M (1991) A low-cost, high-efficiency solar cell based on dye-sensitized colloidal TiO_2 films. Nature 353: 737-740.
2. Yanagida S (2006) Recent research progress of dye-sensitized solar cell in Japan. C R Chim 9: 597-604.
3. Sharifi N, Tajabadi F, Taghavinia N (2014) Recent developments in dye-sensitized solar cells. Comptes Rendus Chimie 15: 3902-3927.
4. Wu M, Ma T (2014) Recent progress of counter electrode catalysts in dye-sensitized solar cells. J Phys Chem C 118: 16727-16742.
5. Yang Y, Zhou CH, Xu S, Hu H, Chen BL, *et al.* (2008) Improved stability of quasi-solid-state dye-sensitized solar cell based on poly (ethylene oxide)–poly (vinylidene fluoride) polymer-blend electrolytes. J Power Sources, 185: 1492-1498.
6. Wu J, Lan Z, Wang D, Hao S, Lin J, *et al.* (2006) Quasi-solid state dye-sensitized solar cells-based gel polymer electrolytes with poly(acrylamide)–poly(ethylene glycol) composite. J Photochem Photobiol A 181: 333-337.
7. Kubo W, Murakoshi K, Kitamura T, Yoshida S, Haruki M, *et al.* (2001) Quasi-solid-state dye-sensitized TiO_2 solar cells: effective charge transport in mesoporous space filled with gel electrolytes containing iodide and iodine. J Phys Chem B 105: 12809-12815.
8. Bella F (2015) Polymer electrolytes and perovskites: lights and shadows in photovoltaic devices. Electrochim Acta 54: 3432-3448.
9. Ohno H (2006) Functional design of ionic liquids. Bull Chem Soc Jpn 79: 1665-1680.
10. Wang Y, Sun Y, Song B, Xi J (2008) Ionic liquid electrolytes based on 1-vinyl-3-alkylimidazolium iodides for dye-sensitized solar cells. Sol Energy Mater Sol Cells 92: 660-666.
11. Zhao Y, Boström T (2015) Application of ionic liquids in solar cells and batteries: A review. Curr Org Chem 19: 556-566.
12. Kim DW, Jeong YB, Kim SH, Lee DY, Song JS (2005) Photovoltaic performance of dye-sensitized solar cell assembled with gel polymer electrolyte. J Power Sources 149: 112-116.
13. Zhang X, Wnag CX, Li FY, Xia YY (2008) A quasi-solid-state dye-sensitized solar cell based on porous polymer electrolyte membrane. J Photochem Photobiol A 194: 31-36.
14. Wei TC, Wan CC, Wang YY (2007) Preparation and characterization of a micro-porous polymer electrolyte with cross-linking network structure for dye-sensitized solar cell. Sol Energy Mater Sol Cells 91: 1892-1897.
15. Chen CM, Shiu HS, Cherng SJ, Wei TC (2009) Preparation of polymer film of micro-porous or island-like structure and its application in dye-sensitized solar cell. J Power Sources 188: 319-322.
16. Kim JH, Jung HS, Park CH, Kang TJ (2014) Porous PVdF-HFP/P123 electrolyte membrane containing flexible quasi-solid-state dye-sensitized solar cells produced by the compression method. J Phys Chem Solids 75: 31-37.
17. Chen HS, Lue SJ, Tung YL, Cheng KW, Ho KC (2011) Elucidation of electrochemical properties of electrolyte-impregnated micro-porous ceramic films as framework supports in dye-sensitized solar cells. J Power Sources 196: 4162-4172.
18. Lue SJ, Lo PW, Hung LY, Tung YL (2010) Application of micro-porous polycarbonate membranes in dye-sensitized solar cells: Cell performance and long-term stability. J Power Sources 195: 7677-7683.
19. Wang P, Klein C, Humphry-Baker R, Zakeeruddin SM, Gratzel M (2005) Stable ≥ 8% efficient nanocrystalline dye-sensitized solar cell based on an electrolyte of low volatility. Appl Phys Lett 86: 123508.
20. Gratzel M (2003) Dye-sensitized solar cells. J Photochem. Photobiol C4: 145-153.
21. Wang P, Zakeeruddin SM, Moser JE, Nazeeruddin MK, Sekiguchi T, *et al.*(2003) A stable quasi-solid-state dye-sensitized solar cell with an amphiphilic ruthenium sensitizer and polymer gel electrolyte. Nat Mater 2: 402-407.
22. Gratzel M (2006) Photovoltaic performance and long-term stability of dye-sensitized meosocopic solar cells. C R Chim 9: 578-583.
23. Flasque M, van Nhien AN, Swiatowska J, Seyeux A, Davoisne C, et al. (2014) Interface stability of a TiO_2/3-methoxypropionitrile-based electrolyte: first evidence for solid electrolyte interphase formation and implications. Chem Phys Chem 15: 1126-1137.
24. Lue SJ, Wang WT, Mahesh KPO, Yang CC (2010) Enhanced performance of a direct methanol alkaline fuel cell (DMAFC) using a polyvinyl alcohol/fumed silica/KOH electrolyte. J Power Sources 195: 7991-7999.
25. Pan WH, Lue SJ, Chang CM, Liu YL (2011) Alkali doped polyvinyl alcohol/multi-walled carbon nano-tube electrolyte for direct methanol alkaline fuel cell. J Membr Sci 376: 225-232.
26. Lue SJ, Pan WH, Chang CM, Liu YL (2012) High-performance direct methanol alkaline fuel cell performance using potassium hydroxide-impregnated polyvinyl alcohol/carbon nano-tube electrolytes. J Power Sources 202: 1-10.
27. Han L, Koide N, Chiba Y, Mitate T (2004) Modeling of an equivalent circuit for dye-sensitized solar cells. Appl Phys Lett 84: 2433-2435.
28. Lue SJ, Wu YL, Tung YL, Shih CM, Wang YC, *et al.* (2015) Functional titanium oxide nano-particles as electron lifetime, electrical conductance enhancer, and long-term performance booster in quasi-solid-state electrolyte for dye-sensitized solar cells. J Power Sources 274: 1283-1291.
29. Lue SJ, Mahesh KPO, Wang WT, Chen JY, Yang CC (2011) Permeant transport properties and cell performance of potassium hydroxide doped poly(vinyl alcohol)/fumed silica nanocomposites. J Membr Sci 367: 256-264.
30. Liberatore M, Decker F, Burtone L, Zardetto V, Brown TM, *et al.* (2009) Using EIS for diagnosis of dye-sensitized solar cells performance. J Appl Electrochem 39: 2291-2295.
31. Wang Q, Moser JE, Grätzel M (2005) Electrochemical impedance spectroscopic analysis of dye-sensitized solar cells. J Phys Chem B 109: 14945-14953.